AD-A169 325 LG WAVE EXCITATION AND PROPAGATION IN PRESENCE OF ONE- 1/1
TWO- AND THREE-DIMENSIONAL HETEROGENEITIES(U) SAINT
LOUIS UNIV MO R B HERRMANN 01 FEB 86 AFGL-TR-86-0026
UNCLASSIFIED F19628-85-K-0029 F/G 8/11 NL

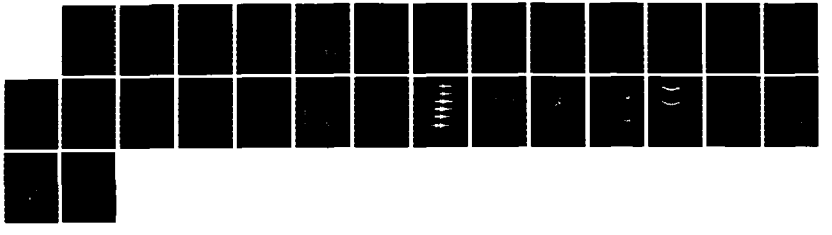

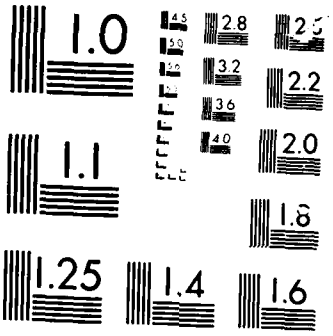
1.0
1.1
1.25
1.4
1.6
1.8
2.0
2.2
2.8
3.2
3.6
4.0

AD-A169 325

(12)

AFGL-TR-86-0026

Lg Wave Excitation and Propagation in Presence of One-, Two-, and Three-Dimensional Heterogeneities

R. B. Herrmann

St. Louis University
221 North Grand Blvd
St. Louis, MO 63103

1 February 1986

Scientific Report No. 2

APPROVED FOR PUBLIC RELEASE; DISTRIBUTION UNLIMITED

DTIC
ELECTE
JUL 1 1986
S D
B

AIR FORCE GEOPHYSICS LABORATORY
AIR FORCE SYSTEMS COMMAND
UNITED STATES AIR FORCE
HANSCOM AIR FORCE BASE, MASSACHUSETTS 01731

DTIC FILE COPY

86 7 1 069

CONTRACTOR REPORTS

This technical report has been reviewed and is approved for publication.

JAMES F. LEWKOWICZ
Contract Manager

HENRY A. OSSING
Chief, Solid Earth Geophysics Branch

FOR THE COMMANDER

DONALD H. ECKHARDT
Director
Earth Sciences Division

This report has been reviewed by the ESD Public Affairs Office (PA) and is releasable to the National Technical Information Service (NTIS).

Qualified requesters may obtain additional copies from the Defense Technical Information Center. All others should apply to the National Technical Information Service.

If your address has changed, or if you wish to be removed from the mailing list, or if the addressee is no longer employed by your organization, please notify AFGL/DAA, Hanscom AFB, MA 01731. This will assist us in maintaining a current mailing list.

Unclassified

SECURITY CLASSIFICATION OF THIS PAGE

ADA 169325

REPORT DOCUMENTATION PAGE

1a. REPORT SECURITY CLASSIFICATION unclassified	1b. RESTRICTIVE MARKINGS
2a. SECURITY CLASSIFICATION AUTHORITY	3. DISTRIBUTION/AVAILABILITY OF REPORT Approved for public release. Distribution unlimited.
2b. DECLASSIFICATION/DOWNGRADING SCHEDULE	
4. PERFORMING ORGANIZATION REPORT NUMBER(S)	5. MONITORING ORGANIZATION REPORT NUMBER(S) AFGL-TR-86-0026
6a. NAME OF PERFORMING ORGANIZATION Saint Louis University 6b. OFFICE SYMBOL (If applicable)	7a. NAME OF MONITORING ORGANIZATION Air Force Geophysics Laboratory
6c. ADDRESS (City, State and ZIP Code) 221 North Grand Boulevard St. Louis, MO 63103	7b. ADDRESS (City, State and ZIP Code) Hanscom Air Force Base, MA 01731
8a. NAME OF FUNDING/SPONSORING ORGANIZATION DARPA/DSO 8b. OFFICE SYMBOL (If applicable) GSD	9. PROCUREMENT INSTRUMENT IDENTIFICATION NUMBER F19628-85-K-0029
8c. ADDRESS (City, State and ZIP Code) 1400 Wilson Blvd. Arlington, VA 22209	10. SOURCE OF FUNDING NOS. PROGRAM ELEMENT NO.: 61101F PROJECT NO.: 5A10 TASK NO.: DA WORK UNIT NO.: AO
11. TITLE (Include Security Classification) Lg Wave Excitation and Propagation (OVER)	
12. PERSONAL AUTHOR(S) R.B. Herrmann	
13a. TYPE OF REPORT Scientific Report 2 13b. TIME COVERED FROM 10/1/85 TO 3/31/86	14. DATE OF REPORT (Yr., Mo., Day) 86 FEB 01 15. PAGE COUNT 26
16. SUPPLEMENTARY NOTATION	
17. COSATI CODES FIELD / GROUP / SUB. GR.	18. SUBJECT TERMS (Continue on reverse if necessary and identify by block number) Lg attenuation and source estimates

19. ABSTRACT (Continue on reverse if necessary and identify by block number)

A detailed study of Lg wave excitation and propagation from a sequence of earthquakes in New Brunswick is performed. Primary conclusions are that Lg Q increases with frequency. Perhaps more importantly for regional source studies is the observation of significant high frequency Pn and Sn arrivals at 1000 km which are much greater than the Lg arrival. Source estimates based on the Lg provide reasonable estimates of seismic moment, but corner frequencies differ from short distance measurements.

20. DISTRIBUTION/AVAILABILITY OF ABSTRACT UNCLASSIFIED/UNLIMITED ☐ SAME AS RPT. ☒ DTIC USERS ☐	21. ABSTRACT SECURITY CLASSIFICATION Unclassified
22a. NAME OF RESPONSIBLE INDIVIDUAL James F. Lewkowicz	22b. TELEPHONE NUMBER (Include Area Code) (617) 377-3028 22c. OFFICE SYMBOL AFGL/LWH

DD FORM 1473, 83 APR EDITION OF 1 JAN 73 IS OBSOLETE.

unclassified

SECURITY CLASSIFICATION OF THIS PAGE

Cont. of Block 11:

in Presence of One-, Two-, and Three-Dimensional Heterogeneities

QUALITY INSPECTED 1

DTIC ELECTE JUL 1 1986 S D B

A-1

TABLE OF CONTENTS

Introduction	1
Spatial Attenuation	1
Spectral Attenuation	3
Corner Frequencies and Seismic Moment	4
Discussion	5
Acknowledgements	6
References	6

LIST OF TABLES

1.	Earth Model for Synthetic Lg	9
2.	Earthquake Catalog Parameters	10
3.	Source Parameters	11

LIST OF FIGURES

1. Distribution of ECTN Stations & Location of the Miramichi Source Zone. 12

2. Comparison of Lg Geometrical Spreading Made by Regressing Peak Amplitudes of the Synthetic Data Set With Distance Using Time Domain, Top, and Smoothed Spectral Amplitudes in the Frequency Domain, Bottom, as a Function of the Butterworth Filter Center Frequency. 13

3. Digital Data From the Station WBO for Event No. 5. The Broadband Signal is Given in the Top Trace, While the Filtered Traces are Shown Below. 14

4. Lg-Q Values Determined From Time Domain (a) and Frequency Domain (b) Analysis. 95% Confidence Limits are Given. 15

5. Lg-Q Values From Time Domain. Circles Represent Use of Data at All Distances, Asterisks the Use of Data at Distances Less than 600 km, and the Diamonds the Use of Data Corrected for the Sn Coda. 16

6. Displacement Spectral Ratio of Event No. 1 to Event No. 3 Recorded at Stations EBN (a) and LPQ (b). The Arrows Indicate the Corner Frequencies and the Solid Line an f^{-2} Trend. The Vertical Scale is in Arbitrary Units. 17

7. Example of a Semilog Plot of Acceleration Spectra at Station GNT for Events No. 3 and 5. The Solid Line Indicates the Mean Slope Corresponding to Q=1853 for This Station. The Slope is Determined Using Data in the 3.0 - 8.0 Hz Range. 18

8. Map Showing the Source Region, Star, and the High Frequency Q Determined for Each Station, Which is Plotted Adjacent to the Station Location. 19

9. Plot of Lg Corner Frequency, f_c, Versus Seismic Moment, M_o, for the Events Studied. The Scaling Laws Proposed by Nuttli (1983) and Hasegawa (1983) are Shown for Comparison. 20

10. Plot of Seismic Moment, M_o, Versus m_{Lg}. The Circles are the ECTN Catalog Values and the Asterisks are Those Determined in This Study. In Addition, the Nuttli (1983) Scaling Law for Mid-plate Earthquakes and the Hasegawa (1983) Relation for Eastern Canada are Given. 21

Lg Attenuation and Source Studies using 1982 Miramichi Data

by T.-C. Shin and R. B. Herrmann

Abstract

Using data from earthquakes in the 1982 Miramichi earthquake source zone, spectral excitation and attenuation of the Lg phase is studied. With data in the distance range of 135 to 994 km, interpretation is complicated by the presence of high frequency Sn and Pn waves which interfere with the Lg wave. At the larger distances, the signal at frequencies above 7 Hz is completely dominated by the non-Lg arrivals. A frequency dependent Lg-Q is determined which rises from 300 at 0.5 Hz to about 1400 at 10 Hz at which it flattens at higher frequency. The Sn coda apparent Q rises above 3000 at frequencies higher than 10 Hz. Seismic moment and corner frequency estimates are made using Lg-Q corrected spectra. The moment estimates compare well with those obtained from long period surface waves and short distance spectral estimates. The Lg corner frequency estimates are substantially lower than the short distance estimates. This discrepancy is the subject of discussion, but the Lg moment-corner frequency estimates do model observed data well when using a Brune (1970) source model and the derived attenuation relation.

INTRODUCTION

The 1982 sequence of earthquakes near Miramichi, New Brunswick has been the subject of many studies (Choy *et al.*, 1983; Cranswick *et al.*, 1982; Mueller and Cranswick, 1985; Saikia and Herrmann, 1985; Wetmiller *et al.*, 1984) which discuss earthquake locations, focal mechanism and source dynamics based on teleseismic and local observations. Regional data are also available from stations of the Eastern Canada Telemetered Network (ECTN) at distances of 135 to 994 km from the focal region.

The ECTN is a digitally telemetered network consisting of vertical component instruments with a system velocity sensitivity that is essentially flat between corner frequencies of 1.0 and 16.0 Hz (Hasegawa, 1985). Data from the ECTN have previously been used to estimate seismic moments and corner frequencies of eastern Canada earthquakes (Hasegawa, 1983) and to study Lg-wave attenuation (Hasegawa, 1985). Hasegawa (1985) used earthquakes with travel paths to ECTN stations that were within or along the edge of the Canadian shield. Data paths for sources in the east in the structurally complex Appalachian province were excluded from his study. The purpose of this present study is to use ECTN data to examine the Lg-wave attenuation for those paths excluded by Hasegawa (1985) and then to compare results.

SPATIAL ATTENUATION

Figure 1 is a map of eastern Canada showing the location of the Miramichi source region and the sites of the ECTN stations used in the study. The ECTN data are acquired at 60 samples a second. Since this study is interested in the frequency dependent excitation and attenuation of the Lg signal, the observed signals are filtered through fifteen different Butterworth bandpass filters whose high- and low-frequency responses fall and rise, respectively, at 24 db/octave. The filter center frequencies were in the range from 0.5 to 15.0 Hz and the filter bandwidth was taken to be 0.7 times the center frequency.

The Lg spatial data are fit by a model of the form

$$A(r) = A_0 \, r^{-n} \, e^{-\gamma r} \tag{1}$$

where n is a coefficient that is taken to be $n = 5/6$ for Lg time domain measurements and $n = 1/2$ for frequency domain measurements. The parameter γ is related to Q by

$$\gamma = \frac{\pi f}{QU} \tag{2}$$

where f is the frequency and U is the group velocity of the wave propagation, taken to be 3.5

km/sec.

To process the data, different approaches were used for time and frequency domain measurements. The time domain study is performed by applying a recursive digital Butterworth filter to the data, and peak amplitudes are read in the time window corresponding to the Lg arrival. To make frequency domain measurements, a 17.07 second time window, corresponding to 1024 time domain samples, is used about the expected Lg arrival. The signal is Fourier transformed, the instrument response removed, and the amplitude spectra at the desired center frequency is obtained by averaging the amplitude spectra between the two corner frequencies of filter.

To test the methodology for interpretation, we synthesized the vertical component Lg-wave at each seismograph station by adding up all higher mode surface waves for the earth model of Table 1. A source depth of 5 km, a focal mechanism with 60^0 dip, 100^0 slip and 200^0 strike were assumed. Synthetic seismograms were generated at a sampling interval of 60 samples per second. Three sets of synthetics were generated corresponding to source corner frequencies of 1, 2 and 3 Hz. The signals included the ECTN instrument response in order to make the synthetics comparable to the actual observed ECTN data. The same processing steps are then applied to the data sets. Approximately 700 seconds of time history were synthesized at each station.

The first test was to measure the peak Lg amplitude as a function of distance for each earthquake using the synthetics generated for a perfectly elastic model. Equation (1) is then used with $\gamma = 0$ to determine the coefficient n. This exercise led to an $n = 0.834$, which is in agreement with previous assumptions (Nuttli, 1973) about the spatial decay of the broad band Lg wave. The next step involved the use of the bandpass filtered signals. Figure 2 presents the geometrical spreading factors n obtained from the smoothed spectral estimates and the filtered time domain signals. The solid horizontal lines indicate the values of $n = 5/6$ for the time domain and $n = 1/2$ for the frequency domain studies. The errors arise from the fact that Lg wave amplitudes do not vary in a uniform manner with distance and because radiation pattern effects for the focal mechanism used can cause azimuthal amplitude variation not accounted for by the model. From this exercise, we conclude that the bandpass filters used are not really so narrow that time domain geometrical spreading cannot be used for the recursively filtered data. This is really expected from surface wave theory because the additional time domain decay is really due to the increasing duration of the signal with distance, and this will also be apparent in the signals filtered as described here.

The geometrical spreading of the filtered time domain data is not exactly the $n = 5/6$ expected for time domain data. However, considering the error bars, we will use the $n = 5/6$ for the filtered time domain signal. If the actual geometrical spreading is somewhat less, this will mean that the inferred γ value is somewhat low and the corresponding Q value somewhat high.

Table 2 gives the epicentral coordinates, identification code, and ECTN published magnitude for each event studied. The range of data covers over three units in short period magnitude, making the data set an excellent one for analysis.

Prior to performing any detailed analysis it is essential that the data be examined. Data at short distances were as expected, with the Lg arrival being the largest signal in all frequency bands. However, we observed an interesting phenomena at distances greater than 500 km. Figure 3 illustrates an this feature of the data for the recording of event No. 5 at the station WBO, an epicentral distance of 702 km from the source. The top trace gives the broadband data, while the other traces are narrow band pass filtered at the indicated center frequencies. The peak Lg arrival is indicated by the arrow at the top of the figure. The Lg arrival is distinct at the low frequencies, but quickly disappears within the mantle Sn coda, which is itself riding on top of the mantle Pn coda. The implication of this observation, is that we can not arbitrarily window the trace about the Lg arrival and expect the spectrum to tell us everything about the Lg at all frequencies. With this particular signal, we can only use frequency up to 7.0 Hz if we are able to determine how much the Lg rises above the coda of the Sn.

Equation (1) is easily linearized and adapted to multiple events. The regression analysis yields a single value of γ, which is related to Q by (2), and an A_0 term for each event proportional

to the source excitation at each filter center frequency. The inferred Q values from the time domain and frequency domain measurements using *all data* at *all distances* are shown in Figure 7. The Q estimates made in each domain agree with each other. The dependence of Lg-Q with frequency can be approximately modeled by the relation $Q(f) = (500\text{–}550)f^{0.65}$. An examination of the data indicates a distinct change in the frequency dependence of Q at about 7 Hz. Above this frequency there is a definite linear trend, while below this frequency there is a suggestion that the Lg Q is attempting to flatten at higher frequencies.

Because of the observation that the Lg arrival time window is contaminated by the Sn and Pn coda at higher frequencies and large distances, the Q values given above are suspect above 7 Hz. To resolve this mixture of time domain data types, two approaches were taken. The first used the data at all distances for frequencies less than 7 Hz, and data acquired at distances less than 600 km for the higher frequencies. These Q values are shown as the squares for low frequencies and as the asterisks at higher frequencies in Figure 5. The circles in Figure 5 are the time domain results shown in Figure 4a. The asterisks have large 95% confidence limits because of the reduced distance coverage. The asterisks support the flattening of Q(f) at higher frequency suggested by the low frequency data.

The second approach attempts to use the Lg data at larger distances by estimating the Lg amplitude. To do this we consider the envelope of the Lg arrival to be sitting upon a predictable envelope of the Sn arrival and its coda. We fit the Sn coda shape using an Aki and Chouet (1975) body-wave scattering model. Subtracting the estimated coda envelope from the observed envelope permits an estimate of the peak Lg amplitude. The modified data set is used in the regression analysis to yield the Q estimates given by the diamonds in Figure 5. This approach yields Q values at higher frequencies intermediate between the other two estimates.

SPECTRAL ATTENUATION

Anderson and Hough (1984) presented an interesting discussion of modeling the high frequency falloff of acceleration spectra in which they showed that a linear trend was observable if a semi-logarithmic plot of acceleration spectra as a function of frequency is made. This linear trend indicates that at high frequencies the acceleration spectra can be modeled by an exponential decay operator. They further found that the exponential decay increased with distance which could be explained by a distance independent site effect and a distance dependent propagation effect.

The acceleration spectra A(f) can be parametrically described by combining a Brune (1970) source spectrum and an attenuation operator as

$$A(f) = \frac{A_o}{1 + (f_c/f)^2} e^{-\pi f t/Q} \tag{3}$$

where f_c is the corner frequency, t is the travel time of the arrival, and Q is the apparent propagation Q. If the model is correct, then a semi-logarithmic plot of A(f) vs f will exhibit a linear trend at frequencies greater than the corner frequency. If the model is incorrect, the data may exhibit an apparent linear trend if only a narrow range of frequencies is considered. One way to test the appropriateness of the Brune (1970) model is to form the spectral ratio of two events at the same distance. The common attenuation effect divides out, and the resulting ratio will exhibit a f^{-2} trend between the corner frequencies if the event with the higher corner frequency has a lower displacement spectral level at high frequencies, which is usually the case. The f^{-2} trend is a direct consequence of the model. Figure 6 compares the displacement spectral ratios of events 1 to 3 at EBN, 135 km, and LPQ, 257 km, from the source zone. The solid line indicates an f^{-2} trend and the arrows indicate the corner frequencies estimated by fitting the A_0 source terms of the regression analysis to a Brune (1970) spectrum. The vertical axis is plotted in arbitrary units and no correction has been made for noise. The noise level for the smaller earthquake is equivalent to the signal level at frequencies less than 0.5 Hz. This exercise indicates that the omega-squared spectral model is reasonable, although the plots are not overwhelmingly convincing.

Figure 7 shows the results of processing the acceleration spectra of events 3 and 5 at the

station GNT. The straight line indicates the inferred linear trend. Based on the appearance of the linear trends, weights were assigned to each slope determination as were windows between which the slopes were to be determined. In this figure, data were used in the 3 - 8 Hz range, and the slope was determined to be -0.0930 $\log_{10}$ units per Hz. If we assume a group velocity of 3.5 km/s to the station, the inferred Q is 1853 using data from 6 events. Figure 8 presents the spectral Q values determined from data at each station. The form of presentation points out the spectral Q determined seems to be very stable for a wide range of epicentral distance. Note that the Q values given here are not directly related to the spatial Q values given in Figures 4 and 5 since a single frequency independent Q value is used to model the spectra. Since this Q is based on the slope which is in turn dependent upon the high frequency spectral level, the spectral Q determined from the slope is more and indication of the high frequency Q rather than a lower frequency Q. We note that the spectral constant Q of about 1900 is within the range of possible Q values near 10 Hz in Figure 5.

CORNER FREQUENCIES AND SEISMIC MOMENT

The ground vertical component Lg-wave displacement spectra, D(f), determined by correcting the observed spectra by the displacement sensitivity of the instrument, at a distance r, is modeled by a relation

$$D(f)=\frac{M_0}{4\pi\rho\beta^3}\frac{S(f)}{r_0}\left(\frac{r_0}{r}\right)^{1/2}e^{-\pi ft/Q} \tag{5}$$

where M_0 is the seismic moment, ρ is the density, β is the crustal shear wave velocity, r_0 is the distance marking a change in signal character from a single body-wave arrival to surface-wave arrivals beyond this point, and S(f) is a normalized Brune displacement source spectrum, given by

$$S(f) = (1+(f/f_c)^2)^{-1}$$

This relation was given by Herrmann and Kijko (1983a) to predict the log-mean spectral level. We use the Hasegawa (1983) values of $r_0 = 100$ km, $\rho = 2.8$ gm/cm^3, and $\beta = 3.8$ km/sec, to apply this relation to eastern Canada. Since we can take $Q(f) = 550f^{0.55}$, approximately, a non-linear inversion technique can be used to use (5) to determine M_o and f_c. Table 3 presents these estimates of these parameters using all available data. The table entries give the event number, the catalog magnitude, M_N, the average f_c and its standard deviation, the log-mean estimate of the seismic moment, obtained by averaging the log moments and then taking the antilog, and the multiplicative confidence factor EM_0 to which the moments are known. The last column, N_s, gives the number of spectra used in the estimation.

In addition to listing the parameters f_c and M_0 which describe the observed data, estimates of source radius, r_0 and stress drop, $\Delta\sigma$, are given using the Brune (1970) relations

$$r_0 = \frac{2.34\beta}{2\pi f_c}$$

and

$$\Delta\sigma = \frac{7M_0}{16r_0^3}.$$

We also derived an m_{Lg} magnitude by low pass filtering the ECTN trace to simulate a seismometer-galvanometer system with a 1.0 Hz seismometer and a galvanometer with 0.8 critical damping and a 1.5 Hz natural frequency. In order to truly model a WWSSN short period system, another lowpass filter at 3.0 Hz would be required to model the effect of the Benioff seismometer inductance, the equivalent response of the simulated seismograms is sufficiently similar to that of the WWSSN short period instrument to be used in determining the m_{Lg} magnitude. We use the m_{Lg} definition of Herrmann and Nuttli (1982)

$$m_{Lg}(f) = 2.94+0.833\log_{10}(r/10) + 0.4342\gamma r + \log_{10}A(r,f). \tag{6}$$

where r is the epicentral distance in km, A is the reduced ground amplitude in microns at

frequency f, and γ is the regional spatial Lg attenuation coefficient and here equals 0.00183 km^{-1} at 1.5 Hz. Herrmann and Kijko (1983b) showed that this relation can be used with instruments other than the WWSSN short period if used as described. The values of the computed m_{Lg} are also given in Table 3, and can be compared to the ECTN catalog values. The computed m_{Lg} values have standard deviations varying between 0.16 and 0.22 magnitude units.

An independent check of the derived sesimic moments was made by comparing the source terms determined from the regression of the frequency domain Lg spectra against distance. There was good agreement. We also corrected each spectra for Q(f), equalized for surface wave geometrical spreading, and determined an RMS average amplitude spectrum. These agreed very well with the spectra predicted for the source parameters of Table 3.

Figure 9 compares the seismic moment - corner frequency values determined in this study with a scaling law proposed by Nuttli (1983) and with observed scaling on the Canadian Shield that Hasegawa (1983) obtained using ECTN data. Figure 10 plots the seismic moment versus magnitude values. The circles use the ECTN catalog magnitudes and the asterisks use the m_{Lg} values determined in this study. The Nuttli (1983) proposed scaling law and the empirical Hasegawa (1983) scaling laws are shown for reference.

DISCUSSION

This paper has presented a number of source parameter and attenuation estimates that must be evaluated in light of other studies. The seismic moment estimates are quite acceptable. Nguyen (1985) determined a seismic moment of 5.9×10^{23} dyne-cm for event 1 by performing a simultaneous inversion for focal mechanism, focal depth and seismic moment from long period Love- and Rayleigh-wave data recorded in North America. This agrees well with our Lg estimate of 5.6×10^{23} dyne-cm. Saikia and Herrmann (1985) modeled three component time history data from data within 10 km of the source of event 3, and estimated the seismic moment to be in the range of $3.3 - 4.1 \times 10^{20}$ dyne-cm, to which our estimate 5.9×10^{20} dyne-cm agrees well. Some of the events of this study also provided locally recorded data analyzed by Mueller and Cranswick (1985). These were events 3, 11, 12, 13 14, 15 and 16. Mueller and Cranswick (1985) used spectral techniques to estimate the seismic moments, corner frequencies and stress drops. Keeping in mind that our seismic moments for events 11 through 16 were based on only one vertical component spectra, the agreement of the estimates is quite good. Our estimates are usually less than a factor of 2 greater than theirs, the only exception being event 15 for which our moment is approximately 2.5 to 3 times greater than theirs. This comparison of Lg seismic moment estimates with other independent estimates points out the stability of Lg seismic moment estimates when care is taken to account for anelastic attenuation.

The value of using Lg-wave corner frequency estimates to infer source properties is currently the subject of considerable discussion (Mueller and Cranswick, 1985). There seems to be an apparent contradiction in that the Lg inferred stress drops are usually lower than the comparable estimates using short distance data. We would like to avoid this issue for the present by stating that the combination of a Brune (1970) source spectrum model and an attenuation operator successfully fit *all* observed spectra (Appendix B, Shin, 1985). Using short distance data for event 3, Mueller and Cranswick (1985) found S-wave corner frequencies in the range of 6 - 15 Hz, while Saikia and Herrmann (1985) found values in the range of 15 - 20 Hz for the same data set. The Lg-corner frequency of Table 3 is constrained to be near 3.5 Hz. One major difference in the data sets is that the short distance spectra could not be fit by a Brune (1970) omega-squared spectrum, but rather required high frequency displacement spectrum falloff with frequency greater than f^{-2}, sometimes greater than f^{-6}! To further complicate the comparison of short distance spectral estimates to large distance Lg spectral estimates, Cranswick *et al* (1985) discussed the problems with near surface site resonances, which can either increase or decrease the apparent corner frequency depending upon the resonance frequency. One can argue that the Lg may be the more robust indicator of source properties since it samples more of the focal sphere, it has different angles of incidence at the receiver which may smooth out the resonance effects seen in a single incident ray, and by the fact that its randomness of arrivals avoids the coherence required for resonance. The Lg study does support a higher frequency content in the source than does the Nuttli (1983) scaling

model, as seen in Figure 9.

The attenuation estimates are not without some ambiguity either. We have found that it is difficult to see the Lg wave at high frequencies at large distances for these travel paths crossing into the Canadian Shield because it attenuates faster than the coda following the Sn and Pn (Figure 3). This observation complicates the analysis of Lg-Q but also indicates that high frequency waves can propagate large distances in the upper mantle. This observation is only now being made because of seismographs recording in this frequency range. Our estimate of Lg-Q for the region is given in Figure 5. Until further data are analyzed at high frequency, our preferred model would be to have the Lg-Q rise sharply at low frequencies and then flatten to about 1500-2000 at high frequencies. This would explain the Lg spectral Q of 1800 or so observed at short distances, and would also admit the possibility of the Sn coda overwhelming the Lg at larger distances. The mantle Sn and its coda can be presumed to be a problem only beyond the distance at which Sn first appears. Hasegawa (1985) modeled vertical component acceleration data derived from the ECTN recordings and concluded that the Lg-Q was $Q(f) = 900f^{0.2}$. This estimate, based on a larger data set, but a different set of propagation paths, is within the error bars of our estimates at frequencies greater than 2.0 Hz. The Hasegawa (1985) has better statistical properties because of the wider range of epicentral distances available, whereas this study used 16 earthquakes recorded at 16 stations, with the source receiver distances fixed.

The seismograms we examined indicated a relationship between arrivals expected from wave theory and those due to a scattering mechanism. Following Dainty (1981) the frequency dependence of the observed Lg-Q, $Q_{obs}(f)$, can be expressed as

$$Q_{obs}(f)^{-1} = Q_{abs}^{-1} + (Q_{0,sca}f)^{-1}$$

which states that the observed Q(f) is a superposition of a frequency independent intrinsic, absorptive Q, and a frequency dependent scattering Q. For our data set we would estimate the intrinsic Q to be about 1500-2000 and the Q_0 to be about 600.

ACKNOWLEDGMENTS

The authors wish to thank the Earth Physics Branch, Energy Mines and Resources Canada for providing the excellent digital data used in the study. The special assistance of H. Hasegawa is very much appreciated. The work discussed was done in fulfillment of the Ph. D. degree by the senior author. This work was supported by the U. S. Nuclear Regulatory Commission under Contract NRC-04-81-195-03, by the U. S. Geological Survey under Contract 14-08-0001-21999, and by NSF Grant CEE-8406577.

REFERENCES

Aki, K. and B. Chouet (1975). Origin of coda waves: source, attenuation, and scattering effects, *J. Geophys. Res.* **80,** 3322-3342.

Anderson, J. G. and S. E. Hough (1984). A model for the shape of the Fourier amplitude spectrum of acceleration at high frequencies, *Bull. Seism. Soc. Am.* **74,** 1969-1995.

Brune, J. N. (1970). Tectonic stress and the spectra of seismic shear waves from earthquakes, *J. Geophys. Res.* **75,** 4997-5009.

Choy, G. L., J. Boatwright, J. W. Dewey, and S. A. Sipkin (1983). A teleseismic analysis of the New Brunswick earthquake of January 9, 1982, *J. Geophys. Res.* **88,** 2199-2212.

Cranswick, E., C. Mueller, R. Wetmiller, and E. Senbera (1982). Local multi-station digital recordings of aftershocks of the January 9, 1982 News Brunswick earthquake, *U. S. Geol. Surv., Open-File Rept. 82-777.*

Cranswick, E., R. Wetmiller, and J. Boatwright (1985). High-frequency observations and source parameters of microearthquakes recorded at hard-rock sites, *Bull. Seism. Soc. Am.* **75,**

1535-1567.

Dainty, A. (1981). A scattering model to explain seismic Q observations in the lithosphere between 1 and 20 Hz, *Geophys. Res. Letters* **11,** 1126-1128.

Hasegawa, H. S. (1983). Lg spectra of local earthquakes recorded by the Eastern Canada Telemetered Network and spectral analysis, *Bull. Seism. Soc. Am.* **73,** 1041-1062.

Hasegawa, H. S. (1985). Attenuation of Lg waves in the Canadian shield, *Bull. Seism. Soc. Am.* **75,** 1569-1582.

Herrmann, R. B. and O. W. Nuttli (1982). Magnitude: The relation of M_L to m_{bLg}, *Bull. Seism. Soc. Am.* **72,** 389-399.

Herrmann, R. B. and A. Kijko (1983a). Modeling some empirical Lg relations, *Bull. Seism. Soc. Am.* **73,** 157-162.

Herrmann, R. B. and A. Kijko (1983b). Short-period Lg magnitudes: instrument, attenuation and source effects, *Bull. Seism. Soc. Am.* **73,** 1835-1850. Mueller, C. S. and E. Cranswick (1985). Source parameters from locally recorded aftershocks of the 9 January 1982 Miramichi, New Brunswick earthquake, *Bull. Seism. Soc. Am.* **75,** 337-360.

Nguyen, B. V. (1985). Surface-wave focal mechanisms, magnitudes, and energies for some earthquakes in eastern North America with tectonic implication, *M. S. Thesis,* Saint Louis University, Saint Louis, Missouri.

Nuttli, O. W. (1983). Average seismic source parameter relation for mid-plate earthquakes, *Bull. Seism. Soc. Am.* **73,** 519-536.

Saikia, C. K. and R. B. Herrmann (1985). Application of waveform modeling to determine focal mechanisms of four 1982 Miramichi aftershocks, *Bull. Seism. Soc. Am.* **75,** 1021-1040.

Shin, T.-C. (1985). Lg and Coda Wave Studies of Eastern Canada, *Ph. D. Dissertation,* Saint Louis University, Saint Louis, Missouri (available through University Microfilms, Ann Arbor, Michigan).

Wetmiller, R. J., J. Adams, F. M. Anglin, H. S. Hasegawa, and A. E. Stevens (1984). Aftershock sequences of the 1982 Miramichi, New Brunswick, earthquake, *Bull. Seism. Soc. Am.* **74,** 621-654.

Department of Earth and Atmospheric Sciences
Saint Louis University
P. O. Box 8099
St. Louis, Missouri 63156

Figure Captions

Fig. 1. Distribution of ECTN stations and location of the Miramichi source zone (star).

Fig. 2. Comparison of Lg geometrical spreading made by regressing peak amplitudes of the synthetic data set with distance using time domain, top, and smoothed spectral amplitudes in the frequency domain, bottom, as a function of the Butterworth filter center frequency.

Fig. 3. Digital data from the station WBO for event No. 5. The broadband signal is given in the top trace, while the filtered traces are shown below.

Fig. 4. Lg-Q values determined from time domain (a) and frequency domain (b) analysis. 95 % confidence limits are given.

Fig. 5. Lg-Q values from time domain. Circles represent use of data at all distances, asterisks the use of data at distances less than 600 km, and the diamonds the use of data corrected for the Sn coda.

Fig. 6. Displacement spectral ratio of event No. 1 to event No. 3 recorded at stations EBN (a) and LPQ (b). The arrows indicate the corner frequencies and the solid line an f^{-2} trend. The vertical scale is in arbitrary units.

Fig. 7. Example of a semilog plot of acceleration spectra at station GNT for events No. 3 and 5. The solid line indicates the mean slope corresponding to Q=1853 for this station. The slope is determined using data in the 3.0 - 8.0 Hz range.

Fig. 8. Map showing the source region, star, and the high frequency Q determined for each station, which is plotted adjacent to the station location.

Fig. 9. Plot of Lg corner frequency, f_c, versus seismic moment, M_o, for the events studied. The scaling laws proposed by Nuttli (1983) and Hasegawa (1983) are shown for comparison.

Fig. 10. Plot of seismic moment, M_0, versus m_{Lg}. The circles are the ECTN catalog values and the asterisks are those determined in this study. In addition the Nuttli (1983) scaling law for mid-plate earthquakes and the Hasegawa (1983) relation for eastern Canada are given.

Table 1
Earth Model for Synthetic Lg

d(km)	α (km/sec)	β (km/sec)	ρ (gm/cc)
1	5.00	2.89	2.5
9	6.10	3.52	2.7
10	6.40	3.70	2.9
20	6.70	3.87	3.0
	8.15	4.70	3.4

Table 2

Earthquake Catalog Parameters

No.	Date	Origin time UT	Latitude N°	Longitude W°	M_N
1	11 Jan. 82	21:41:08	46.6	66.6	5.40
3	17 Jan. 82	13:33:56	46.6	66.6	3.50
5	31 Mar. 82	21:02:20	46.6	66.6	5.10
6	04 Apr. 82	13:50:12	46.6	66.6	4.30
7	11 Apr. 82	18:00:53	46.6	66.6	4.00
8	18 Apr. 82	22:47:21	46.6	66.6	4.00
9	06 May 82	16:41:07	46.6	66.6	4.00
10	16 Jan. 82	15:31:22	46.6	66.6	2.06
11	16 Jan. 82	15:53:39	46.6	66.6	3.07
12	17 Jan. 82	14:08:14	46.6	66.6	2.46
13	17 Jan. 82	17:57:40	46.6	66.6	2.08
14	18 Jan. 82	02:58:46	46.6	66.6	2.16
15	19 Jan. 82	11:58:49	46.6	66.6	2.46
16	20 Jan. 82	08:21:38	46.6	66.6	2.16

M_N : Lg magnitude used in ECTN

Table 3

SOURCE PARAMETERS

No.	M_N	m_{Lg}	f_c Hz	Ef_c Hz	M_o dyne-cm ($x10^{22}$)	EM_o	r_0 km	$\Delta\sigma$ bars	N_S
1	5.40	5.73	0.51	0.11	55.80	1.95	2.758	11.646	13
3	3.50	3.74	3.44	0.06	0.059	2.57	0.411	3.719	9
5	5.10	5.00	0.85	0.14	11.17	2.51	1.651	10.857	14
6	4.30	4.47	2.33	0.15	0.49	2.45	0.613	9.327	10
7	4.00	4.24	2.50	0.18	0.17	2.18	0.564	4.003	11
8	4.00	4.23	2.44	0.15	0.18	2.09	0.573	4.127	12
9	4.00	4.18	2.50	0.17	0.18	2.51	0.565	4.571	10
10	2.10		10.20		0.0018		0.136	3.225	1
11	3.00		6.00		0.011		0.236	3.406	1
12	2.46		9.40		0.002		0.151	2.610	1
13	2.16		10.60		0.0014		0.134	2.496	1
14	2.08		10.80		0.0013		0.131	2.465	1
15	2.46		8.60		0.0031		0.165	3.069	1
16	2.16		10.00		0.0011		0.129	2.275	1

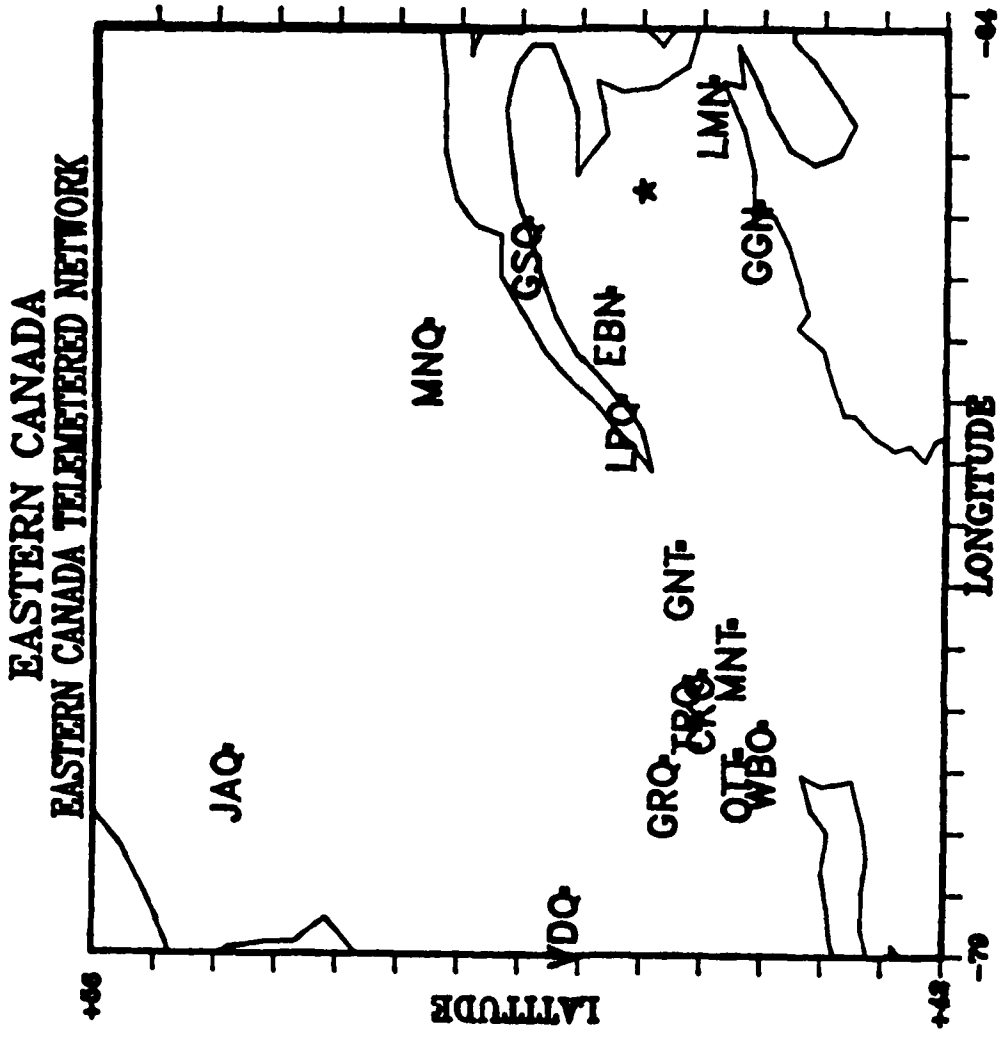

Fig. 1. Distribution of ECTN stations and location of the Miramichi source zone (star).

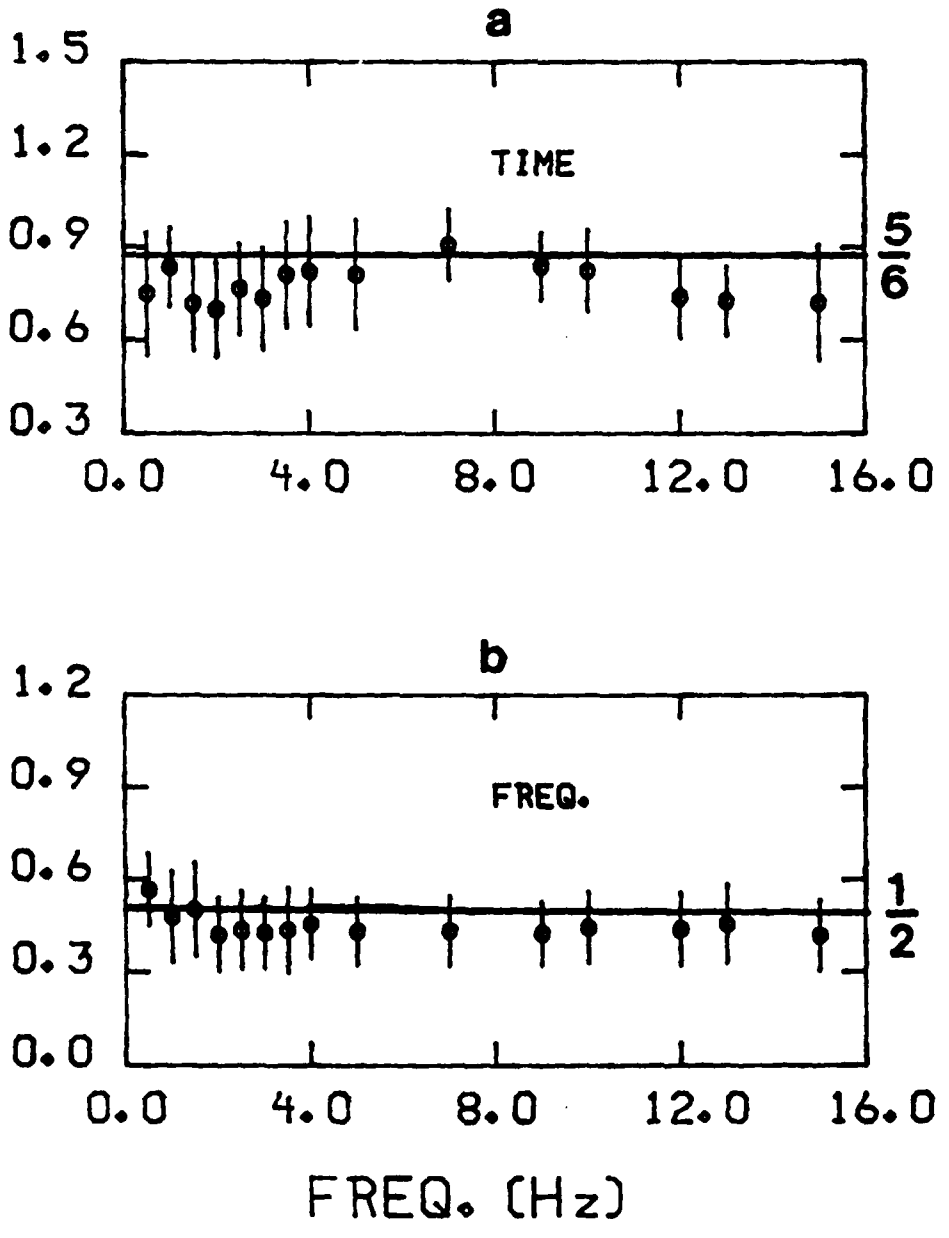

Fig. 2. Comparison of Lg geometrical spreading made by regressing peak amplitudes of the synthetic data set with distance using time domain, top, and smoothed spectral amplitudes in the frequency domain, bottom, as a function of the Butterworth filter center frequency.

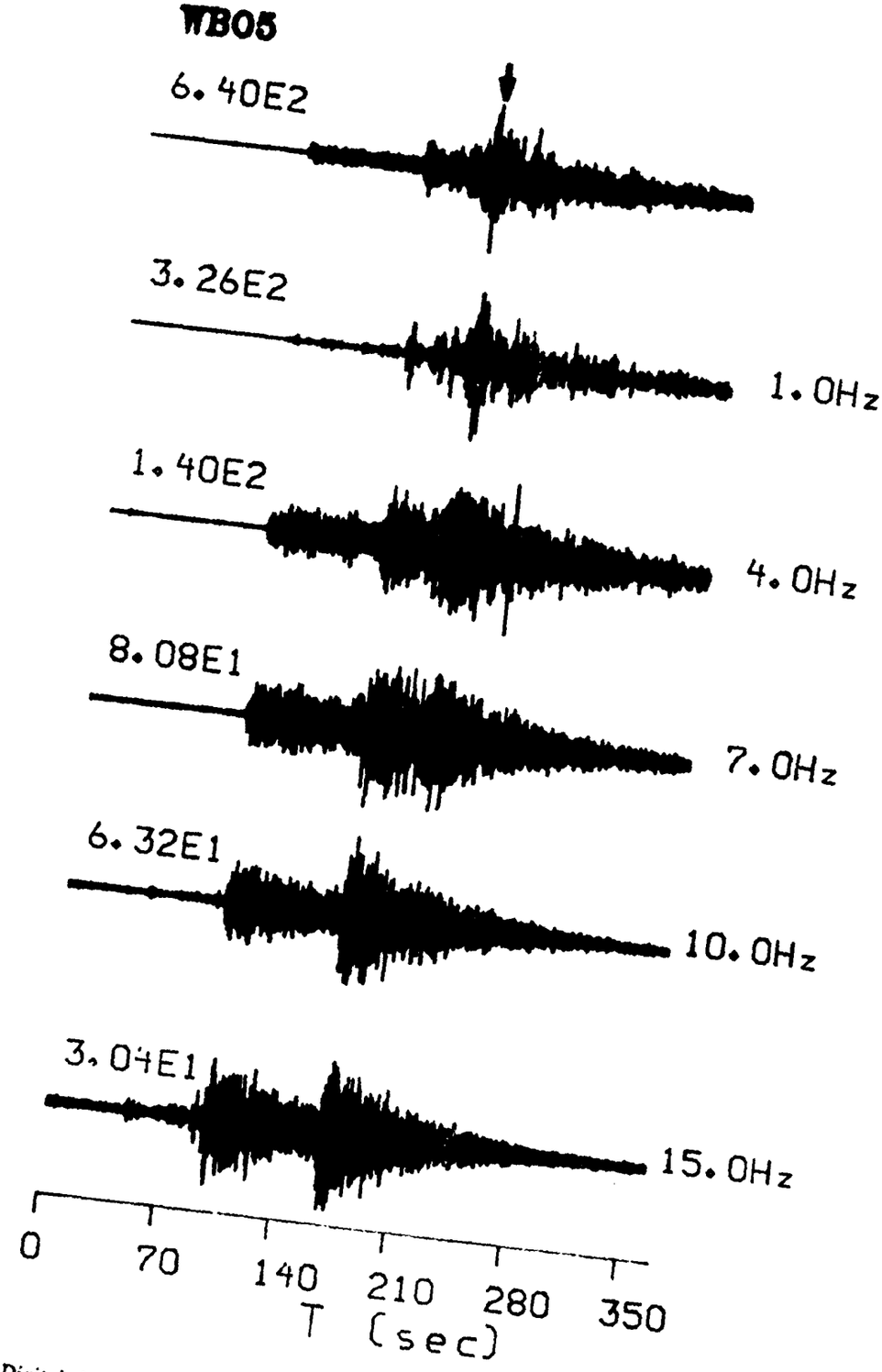

Fig. 3. Digital data from the station WBO for event No. 5. The broadband signal is given in the top trace, while the filtered traces are shown below.

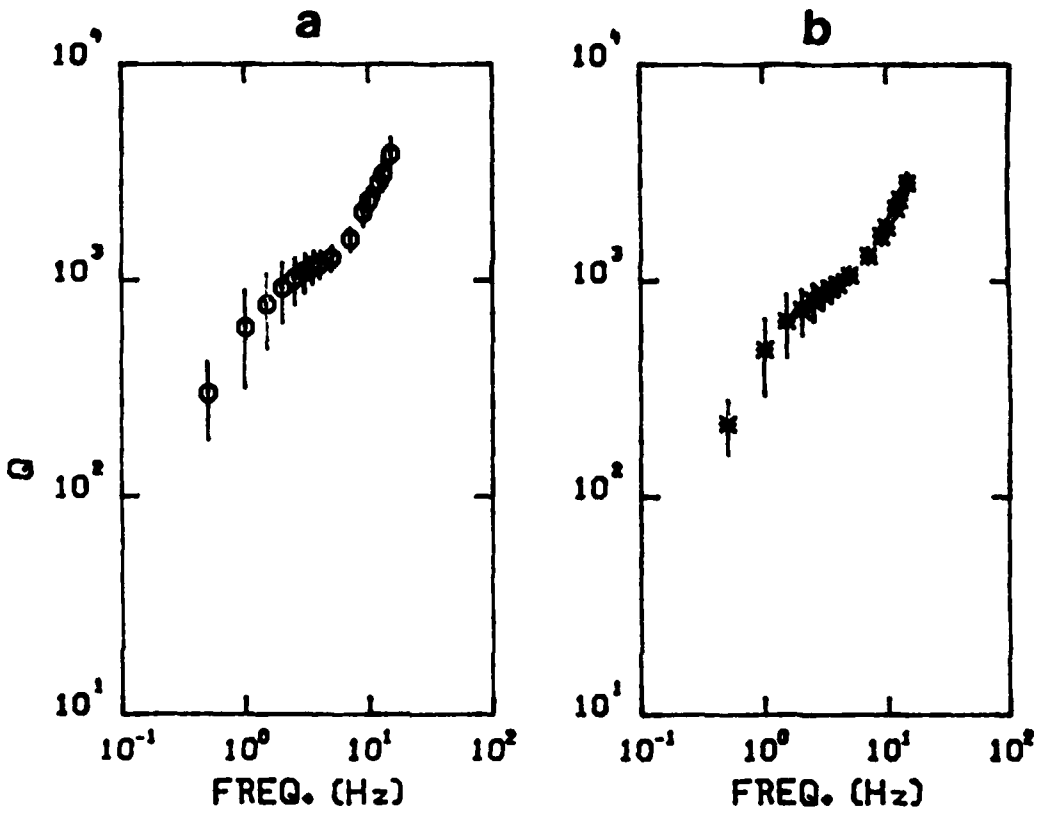

Fig. 4. Lg-Q values determined from time domain (a) and frequency domain (b) analysis. 95 % confidence limits are given.

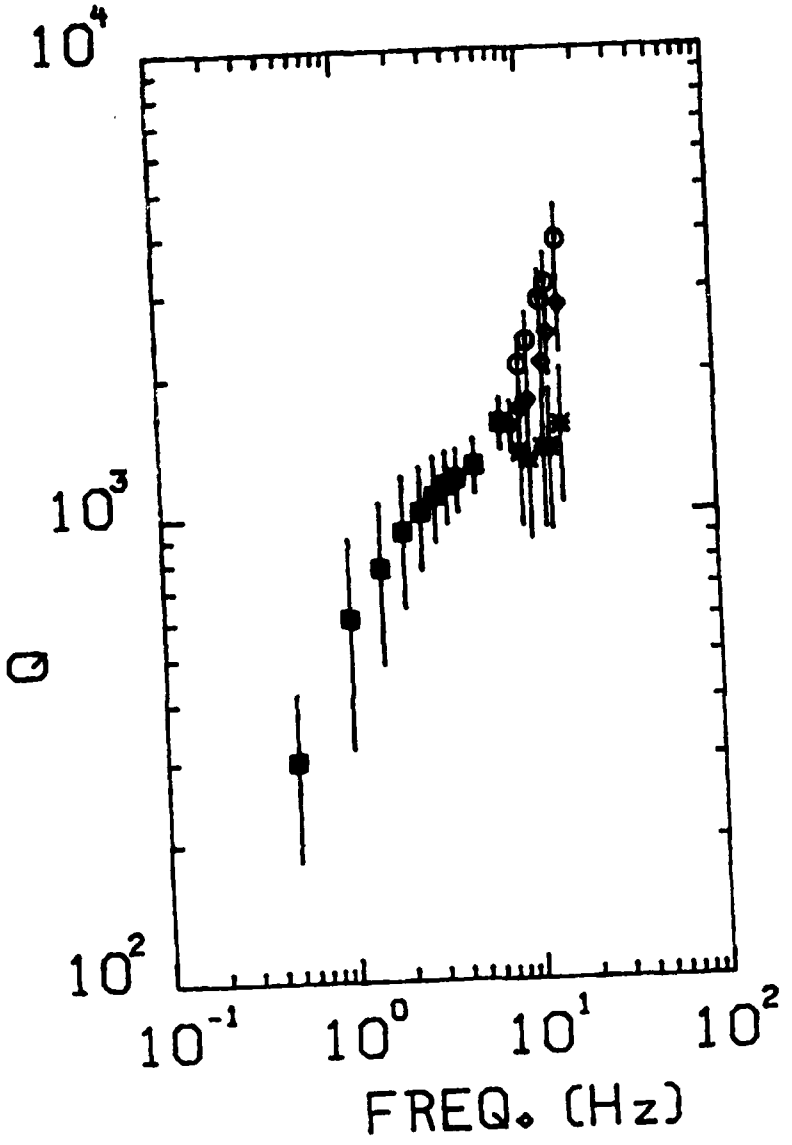

Fig. 5. Lg-Q values from time domain. Circles represent use of data at all distances, asterisks the use of data at distances less than 600 km, and the diamonds the use of data corrected for the Sn coda.

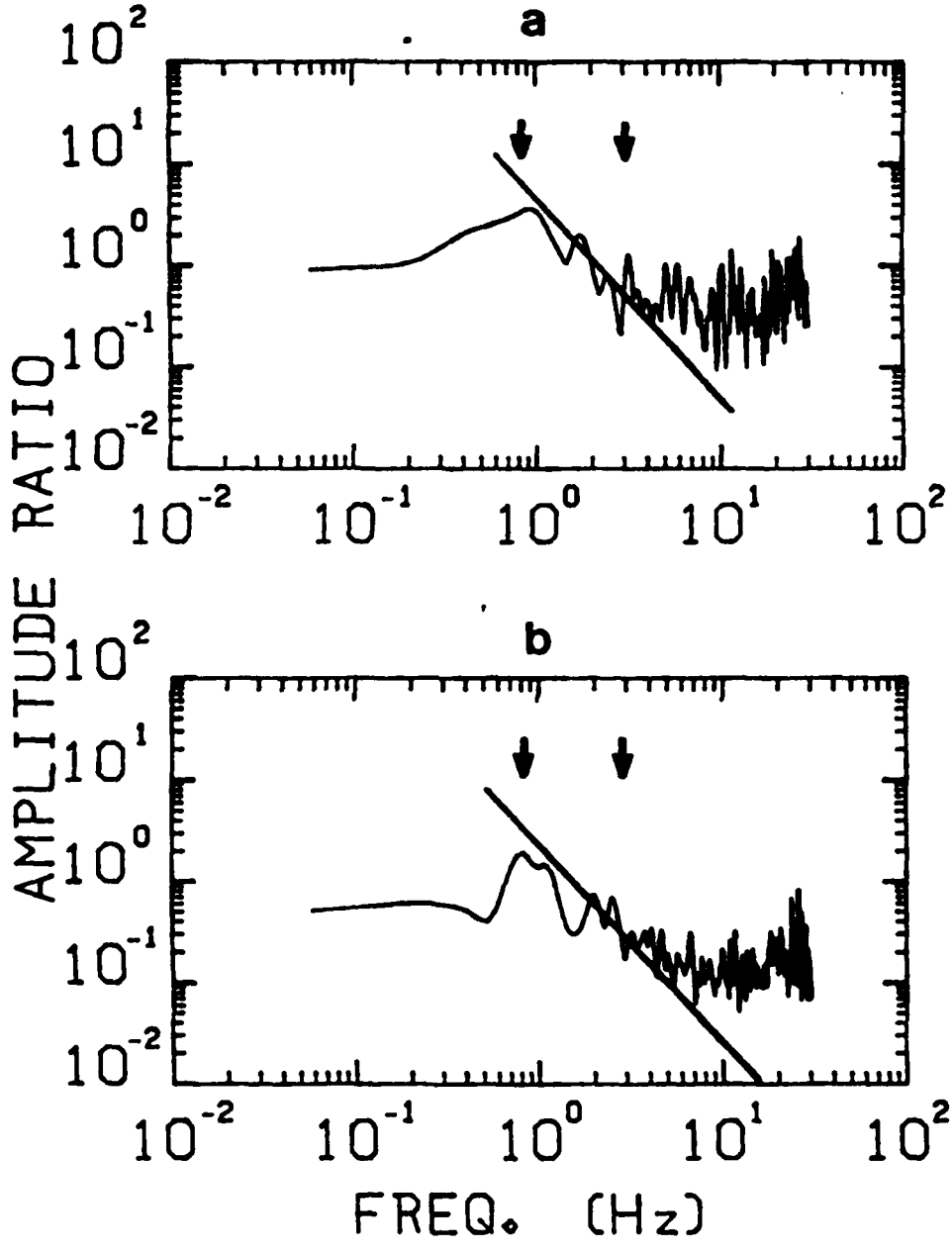

Fig. 6. Displacement spectral ratio of event No. 1 to event No. 3 recorded at stations EBN (a) and LPQ (b). The arrows indicate the corner frequencies and the solid line an f^{-2} trend. The vertical scale is in arbitrary units.

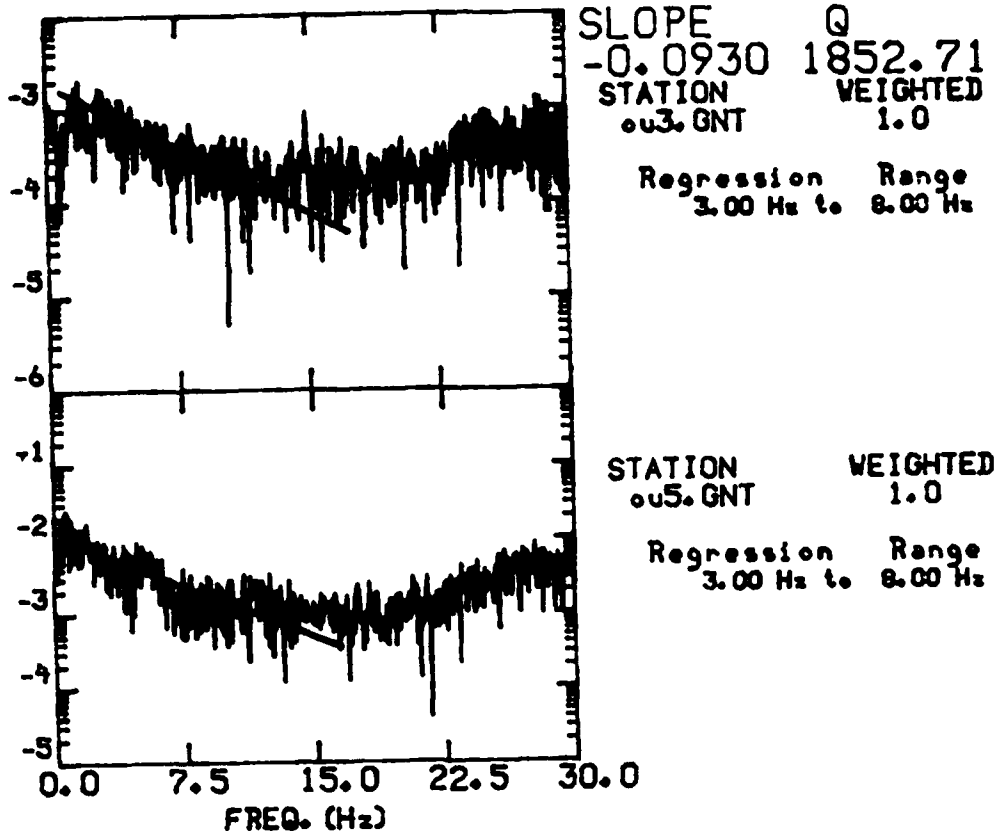

Fig. 7. Example of a semilog plot of acceleration spectra at station GNT for events No. 3 and 5. The solid line indicates the mean slope corresponding to Q=1853 for this station. The slope is determined using data in the 3.0 - 8.0 Hz range.

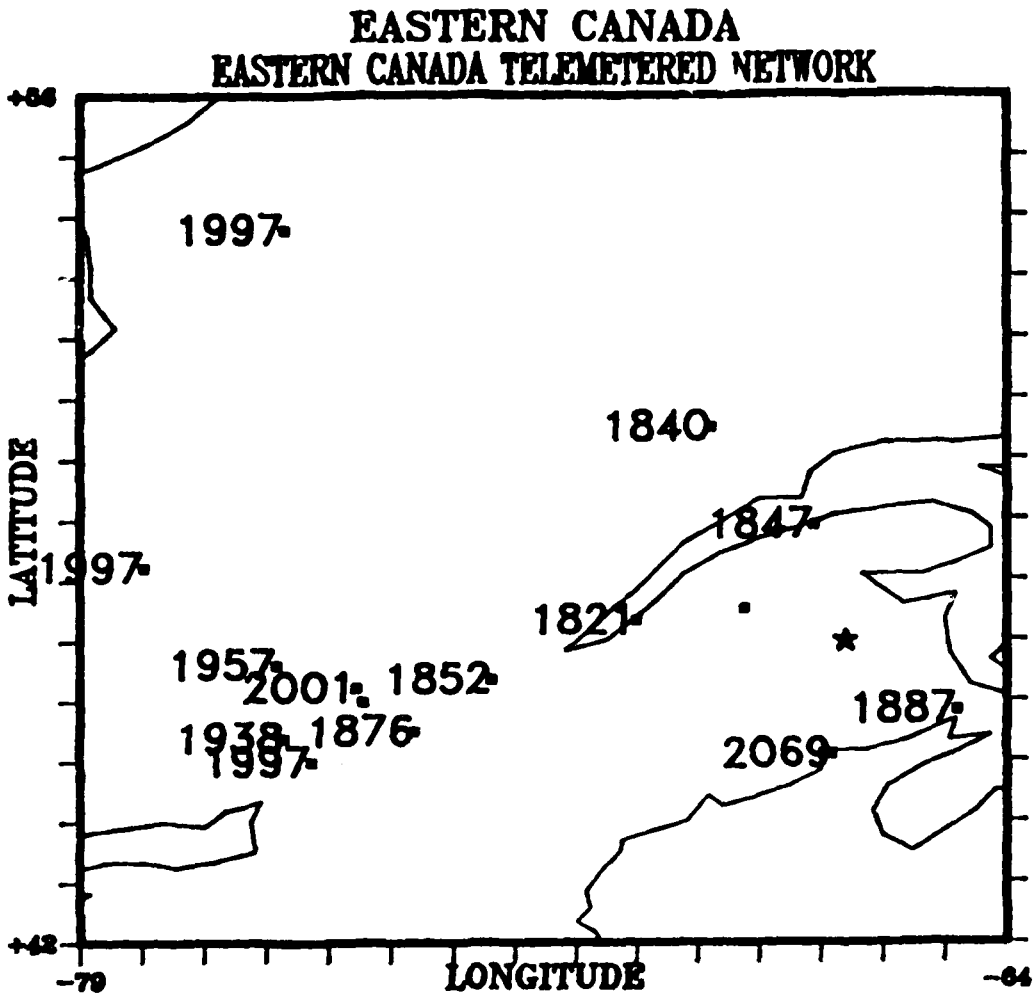

Fig. 8. Map showing the source region, star, and the high frequency Q determined for each station, which is plotted adjacent to the station location.

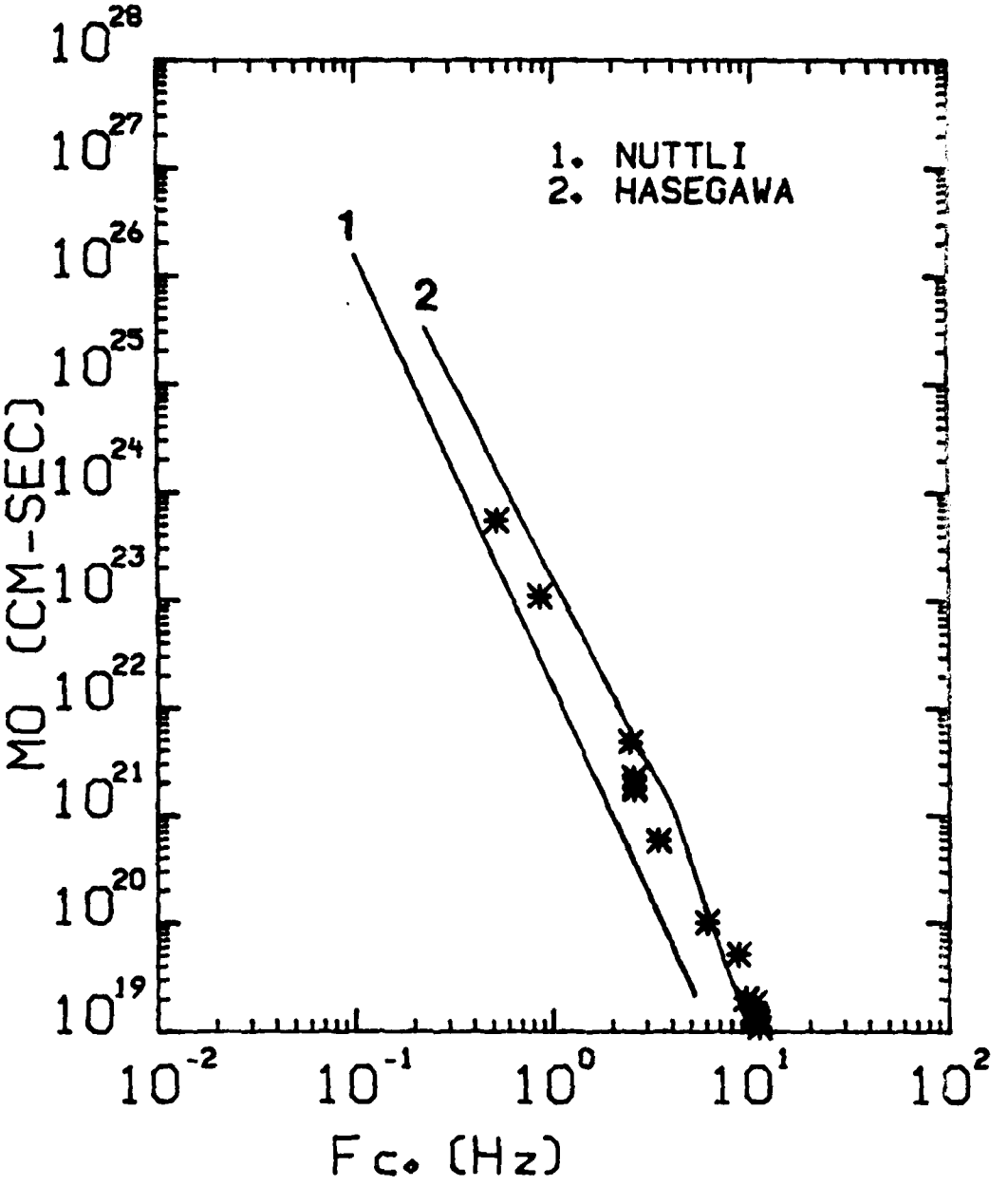

Fig. 9. Plot of Lg corner frequency, f_c, versus seismic moment, M_o, for the events studied. The scaling laws proposed by Nuttli (1983) and Hasegawa (1983) are shown for comparison.

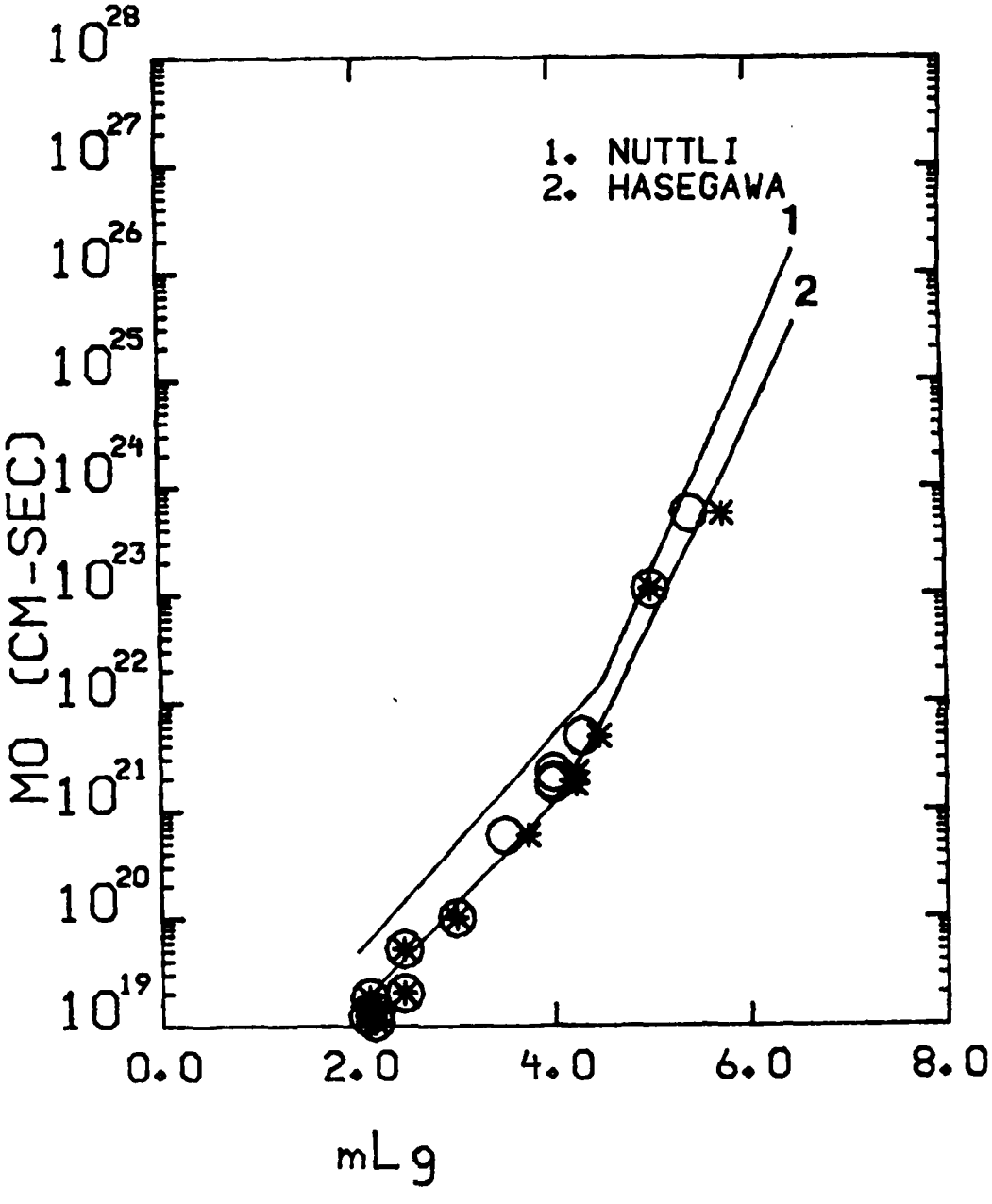

Fig. 10. Plot of seismic moment, M_0, versus m_{Lg}. The circles are the ECTN catalog values and the asterisks are those determined in this study. In addition the Nuttli (1983) scaling law for mid-plate earthquakes and the Hasegawa (1983) relation for eastern Canada are given.

END

DTIC

7-86